Microchimica Acta (2022) 189: 135
https://doi.org/10.1007/s00604-022-05227-3

ORIGINAL PAPER

Heparin-enhanced peroxidase-like activity of iron-cobalt oxide nanosheets for sensitive colorimetric detection of trypsin

Chenyu Zhou[1] · Junyang Chen[1] · Guannan Wang[2] · Xingguang Su[1]

Received: 6 December 2021 / Accepted: 14 February 2022 / Published online: 7 March 2022

Abstract

Iron-cobalt oxide nanosheets (FeCo-ONSs) were proved to have intrinsic peroxidase-like activity. Additionally, the peroxidase-like activity of FeCo-ONSs toward the oxidation of 3,3,5,5-tetramethylbenzidine (TMB) was dramatically enhanced after heparin addition due to the stronger affinity toward TMB. Protamine combines with heparin, so the promotion of peroxidase-like activity of FeCo-ONSs with heparin was suppressed. With the addition of trypsin, protamine was hydrolyzed and the enhancement effect of catalytic activity of FeCo-ONSs was recovered. Based on above process, a sensitive colorimetric platform for trypsin activity determination was constructed through measuring the absorbance of produced oxTMB at 652 nm, providing a linear detection range of 5 to 500 ng/mL and a low detection limit of 2.8 ng/mL. The method was applied to trypsin determination in real samples (human urine sample and multienzyme tablet sample) with satisfactory results, illustrating the potential application of this biosensor.

Keywords Iron-cobalt oxide nanosheets · Colorimetric detection · Trypsin activity · Peroxidase-like activity

Introduction

Trypsin is an important class of proteases and its level is associated with a variety of diseases, such as pancreatitis, meconium intestinal obstruction, and cell apoptosis [1]. In addition, it has recently been linked to the development of neoplasia, as well as the invasion and metastasis of several cancers [2, 3]. As a result, trypsin is regarded as a specific biomarker and the reliable method for trypsin activity detection is of great significance in the treatment of pancreatic diseases and epidemic diseases. Accordingly, several different methods have been developed for trypsin determination, such as chromatography [4], enzyme-linked immunosorbent assay [5], fluorimetry [6, 7], electrochemistry [8], chemiluminescence [9, 10], and surface-enhanced Raman scattering [11]. Even so, more novel, cheap, and sensitive analytical methods for trypsin concentration are highly demanding.

Nanozyme is a type of fascinating nanomaterial with enzyme-like properties. In contrast to natural enzymes, nanozymes are generally low-cost, stable, easy to store, and activity tunable. Hence, nanozymes are considered as promising alternatives to mitigate the limitations of nature enzymes. Moreover, the unique physical and chemical properties of nanozymes not only enable them to have multiple functionalities, but also offer greater possibilities for future applications in numerous research fields, such as biochemical sensing, tumor treatment, organic degradation, and food safety assay [12–16]. Since the intrinsic peroxidase-like activity of magnetic iron oxide nanoparticles was first reported in 2007 [17], various nanomaterials, such as carbon materials [18, 19], metal organic frameworks (MOFs) [20, 21], noble metal nanoclusters [22–24], metal oxide [25–27], and metal sulfide nanomaterials [28], have been found to exhibit the catalytic properties of natural enzymes.

Among all the enzyme mimics, two-dimensional (2D) nanosheets (NSs) with ultrathin structure have been attracting a lot of interest because of their special physical, chemical, and electronic properties. Nanosheets are expected to have the immense potential for high-performance towards the enzyme mimics based on the large surface area and the

✉ Guannan Wang
chemwangguannan@126.com

✉ Xingguang Su
suxg@jlu.edu.cn

[1] Department of Analytical Chemistry, College of Chemistry, Jilin University, Changchun 130012, China

[2] College of Medical Engineering, Jining Medical University, Jining 272067, People's Republic of China

exposure of most atoms on their surface. The two-dimensional carboxy-modified grapheme oxide (GO) nanosheets were first reported to have peroxidase-like activity and successively applied in glucose detection [29]. Later, a large number of 2D nanomaterials have been investigated to have catalytic activities in terms of natural enzymes such as peroxidase, oxidase, and catalase along with diverse applications [30–33]. Although remarkable achievement has been realized in the field of nanozymes research, the low catalytic activity of nanozymes caused by many factors such as low metal atom utilization efficiency, poor environmental stability, or nanozymes aggregation is still an urgent problem to be solved. Because the surface property is closely related to nanozyme activity, surface modification is used as one of the effective methods to regulate the catalytic efficiency of nanozymes. For example, Cai et al. synthesized Au nanoparticle-decorated WSe_2 (Au@WSe_2) hybrid nanozymes which exhibited about twofold higher peroxidase-like activity compared to WSe_2 nanosheets alone [34]. The oxidized glutathione-modified MoS_2 nanosheets prepared by Gu's group have better dispersibility and higher affinity to the substrate TMB, which is beneficial for improving peroxidase-like catalytic activity of MoS_2 [35].

In this work, we successfully prepared iron-cobalt oxide nanosheets (FeCo-ONSs) via a mild solution reduction method using $NaBH_4$ as a reductant, and the prepared FeCo-ONSs have peroxidase-like (POD) activity. To our best knowledge, the peroxidase mimetic activity of the FeCo-ONSs has not yet been reported. Additionally, based on the heparin-triggered enhancement of peroxidase-like activity of FeCo-ONSs with TMB as substrate, we constructed a "signal on–off-on" colorimetric sensing platform for trypsin activity detection. As illustrated in Scheme 1, with the adsorption of negatively charged heparin, the peroxidase-like activity of FeCo-ONSs was enhanced due to the facilitation of the adsorption to TMB. Positively charged protamine could bind with negatively charged heparin via an electrostatic interaction, leading to the heparin-triggered catalytic enhancement of peroxidase-like activity of FeCo-ONSs decreased. After adding trypsin, protamine was hydrolyzed into small fragments, heparin-triggered enhancement of peroxidase-like activity of FeCo-ONSs was recovered, and the TMB oxidation was accelerated again. Thus, trypsin activity can be determined through measuring the absorbance of produced oxTMB at 652 nm.

Experiment section

Materials and apparatus

The details of experimental reagents and apparatus are provided in supporting information.

Preparation of FeCo-ONSs

The FeCo-ONSs were prepared according to an earlier report with some modifications [36]. The synthetic steps are given in supporting information.

Investigation of enzyme mimicking activity of FeCo-ONSs

The peroxidase-like activity of the as-prepared FeCo-ONSs was investigated through typical catalytic oxidation reaction of TMB, o-phenylenediamine (OPD), and 2,2'-azinobis(3-ethylbenzothiazoline-6-sulfonate) (ABTS) in the presence of H_2O_2. A total of 200 μL of acetate buffer (200 mM, pH 3.5), 200 μL of H_2O_2 (100 mM), 200 μL of 250 μg/mL FeCo-ONSs aqueous suspension, and 40 μL of chromogenic substrates (10 mM TMB, 10 mM OPD, 5 mM ABTS) were subsequently added into 1360 μL of deionized water. After

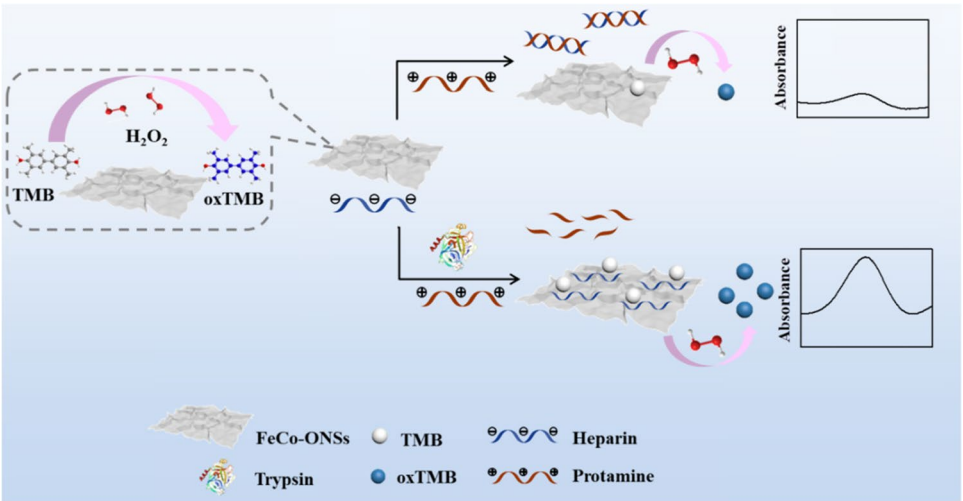

Scheme 1 The mechanism for trypsin detection via the heparin-modulated peroxidase-like activity of FeCo-ONSs

being incubated at room temperature for 40 min, the absorption spectrums of resultant solutions were measured.

Colorimetric biosensing of trypsin

For quantitative analysis of trypsin, 50 µL of trypsin with different concentrations, 50 µL of protamine (200 µg/mL), and 50 µL of Tris–HCl buffer solution (0.2 M, pH 7.8) were added into 350 µL of deionized water, and incubated in 37 °C for 40 min, followed by the addition of 200 µL of heparin (200 µg/mL), 100 µL of acetate buffer (0.2 M, pH 4.5), 80 µL of H_2O_2 (10 mM), 20 µL of TMB (10 mM), and 100 µL FeCo-ONSs (100 µg/mL). The mixed solution was reacted at 20 °C for 25 min. After that, the absorbance at 652 nm of the reacted solution was recorded by ultraviolet–visible absorption spectrophotometry.

Trypsin detection in real samples

Healthy human urine sample was chosen to investigate the applicability of our colorimetric method for trypsin determination in biological samples. The urine sample was obtained from a healthy adult volunteer. Different concentrations (250, 500, 750 ng/mL) of trypsin standard solution were added into the urine sample. The obtained trypsin-spiked urine samples were diluted 5 times and detected as described above.

Multienzyme tablets purchased from a local pharmacy were selected to explore the feasibility of this method for trypsin determination in drug samples. The powder obtained by grinding tablets was dissolved in ultrapure water and treated with ultrasonic for 1 h. Similarly, different concentrations (200, 400, 600 µg/mL) of trypsin standard solution were added into the above drug sample. The obtained trypsin-spiked drug samples were diluted 4000 times and detected in the same way.

Results and discussion

Characterization

The scanning electron microscope (SEM) images in Fig. 1(A) and (B) show that the synthesized FeCo-ONSs displayed an obvious crumpled morphology with large amount of wrinkles, assembled by curly nanosheets. Besides, the transmission electron microscopy (TEM) analysis was implemented, and the TEM images shown in Fig. 1(C, D) obviously illustrated that the FeCo-ONSs are two-dimensional flake structures. To evaluate the crystalline structures of synthesized FeCo-ONSs, X-ray powder diffraction (XRD) characterizations were implemented. As shown in Fig. 1(E), only two weak diffraction peaks at 34.5° and 60.7° were observed in XRD pattern in comparison with the standard structure of $CoFe_2O_4$ (JCPDS No. 22–1086), revealing the low crystallinity of the FeCo-ONSs. FT-IR analysis was carried out to investigate the surface structure. As displayed in Fig. 1(F), the adsorption peaks exhibited at 3409 cm^{-1} and 1635 cm^{-1} were attributed to the stretching and bending vibration of O–H of physically adsorbed water on the FeCo-ONSs, respectively. The peaks at 2919 cm^{-1} and 1105 cm^{-1} were corresponding to the stretching vibration of C = O and $-CH_2$, respectively [37]. The sharp peak appeared at 1382 cm^{-1} responded to the characteristic stretching vibration of residual NO_3^- [38]. The peaks at 478 cm^{-1} and 577 cm^{-1} were correlated with the cobalt-oxygen and iron-oxygen stretching vibration, respectively [38, 39], which indicated the formation of the metal–oxygen bonds in the FeCo-ONSs. All these results demonstrated the successful preparation of FeCo-ONSs with carbonyl groups on the surface.

Peroxidase-like activity of FeCo-ONSs

As a representative chromogenic substrate, TMB was selected to assess the peroxidase mimetic activity of the FeCo-ONSs. As shown in Fig. 2(A), FeCo-ONSs were able to catalyze the oxidation of TMB by H_2O_2 accompanied by a remarkable absorption peak at 652 nm, while the oxidation reaction was much slower and almost no obvious characteristic peak was observed when only H_2O_2 or FeCo-ONSs were present. Aside from the TMB, some other frequently used substrates such as OPD and ABTS could also be oxidized in the presence of FeCo-ONSs and H_2O_2 (Fig. 2(B)). The above results demonstrated that FeCo-ONSs have peroxidase-like performances.

In order to acquire a deep understanding of the peroxidase mimicking activity of FeCo-ONSs, the reaction conditions were optimized and the catalytic mechanism was investigated by a series of experiments. It can be found in Fig. S1(A) that the peroxidase-like activity of FeCo-ONSs obviously varied with pH value changing from 3.0 to 6.0 and exhibited the best activity at pH 3.5. Figure S1(B) shows that the optimal reaction temperature was 45 °C. Then to identify the possible reactive oxygen species produced in the catalysis process, isopropanol (IPA), p-benzoquinone (pBQ), and tryptophan (Trp) were employed as the scavengers to capture hydroxyl radical (•OH), superoxide radical ($O_2^{\bullet-}$), and singlet oxygen ($^1O_2$), respectively [40, 41]. As shown in Fig. 2(C), the absorbance at 652 nm of the system hardly changed after adding the pBQ or Trp, but significantly decreased after the injection of IPA. Moreover, the decreasing effect was more obvious along with an increase in IPA amount. The results illustrated that the hydroxyl radical (•OH) was the main active species for TMB oxidation in the presence of FeCo-ONSs and H_2O_2. Furthermore,

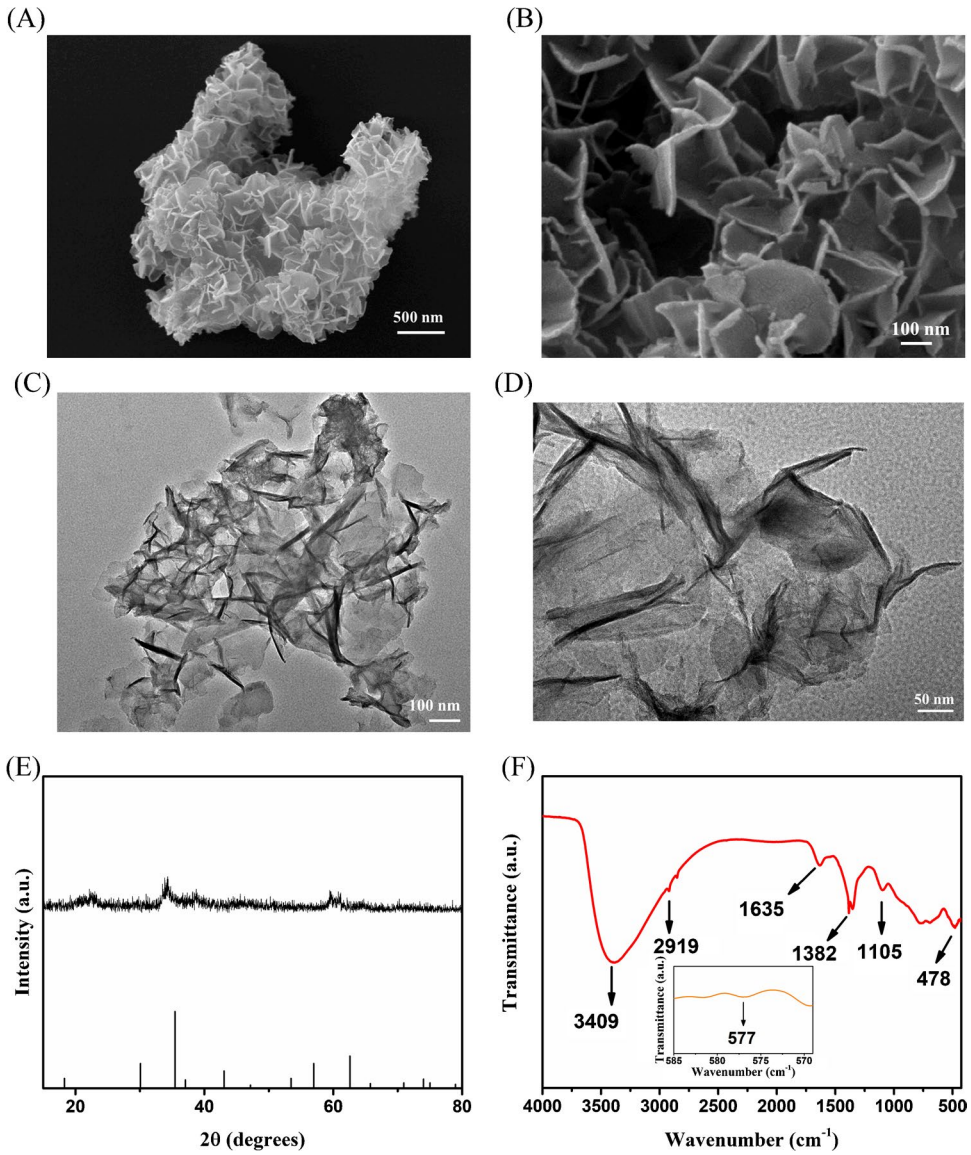

Fig. 1 **A**, **B** SEM images, **C**, **D** TEM images, **E** XRD pattern, and **F** FI-TR spectra of FeCo-ONSs

terephthalic acid (TA) was applied to verify the existence of hydroxyl radical (•OH), since non-fluorescent TA could be oxidized by hydroxyl radical (•OH) to form 2-hydroxy terephthalic acid with high fluorescence [42]. From Fig. 2(D), the distinct fluorescence signal at 426 nm could be clearly found in the TA/H_2O_2/FeCo-ONS system, confirming that the hydroxyl radical was generated during the catalytic oxidation of substrates.

To better evaluate the peroxidase activity of FeCo-ONSs, steady-state kinetic analysis was conducted and the Michaelis – Menten constant (K_m) and maximum velocity (V_{max}) were obtained using Lineweaver–Burk plot (Fig. S2). In general, a lower value of K_m implies a higher affinity between the nanozymes and the substrates. As demonstrated in Table S1, the FeCo-ONSs show pretty lower K_m especially toward H_2O_2 compared to horseradish peroxidase (HRP) and some other nanozymes. This splendid affinity with H_2O_2 may be related to the abundant oxygen vacancies in ultrathin FeCo-ONSs [36]. The interaction between oxygen vacancies and H_2O_2 can generate reactive oxygen species, which oxidize the corresponding substrates [43–45]. Although the K_m value of FeCo-ONSs with TMB as substrate is a little higher than those of HRP and other nanozymes, the K_m value of FeCo-ONSs-heparin is comparable with those of HRP and other nanozymes.

Design and construction of FeCo-ONSs and heparin-based colorimetric system

Interestingly, we discovered that the peroxidase-like activity of FeCo-ONSs toward the oxidation of TMB was significantly enhanced after the addition of heparin. As shown in Fig. 3(A), an obvious enhanced absorption peak of oxTMB at 652 nm was observed in the presence of heparin (curve

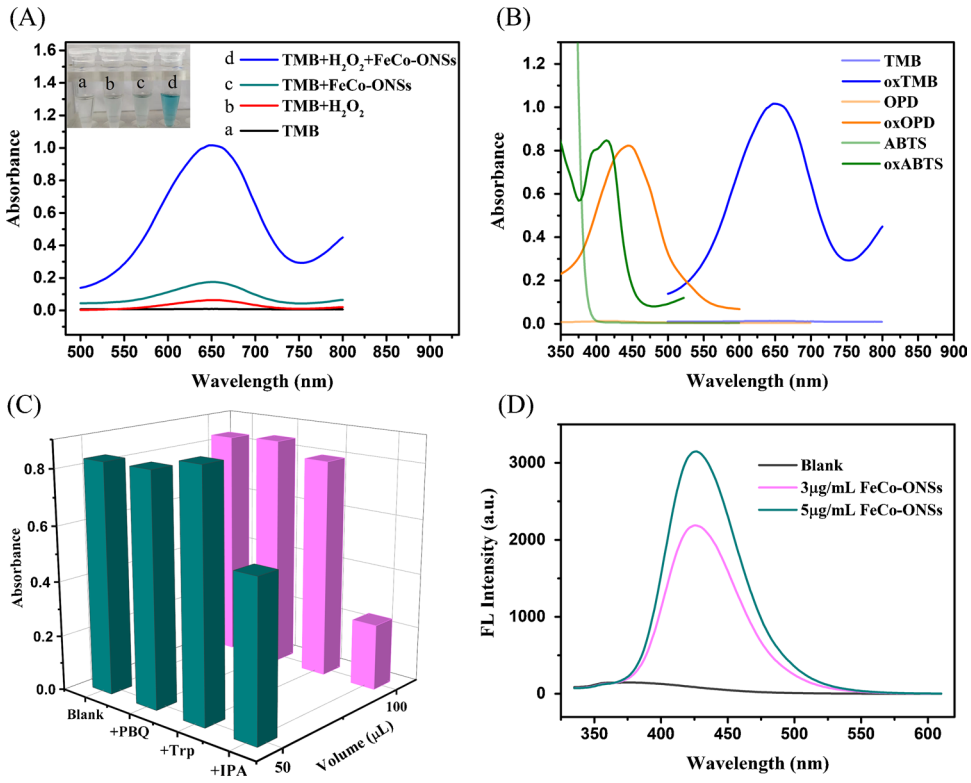

Fig. 2 **A** UV–vis spectra of TMB, TMB/H_2O_2, TMB/FeCo-ONSs, and TMB/H_2O_2/FeCo-ONSs system, respectively. **B** UV–vis spectra of substrates (TMB, ABTS, and OPD) with and without FeCo-ONSs/H_2O_2, respectively. **C** Effects of three scavengers with different amounts on FeCo-ONS-catalyzed oxidation of TMB by H_2O_2 (PBQ: 1 mM; Trp: 2.5 mM; IPA ≥ 99.7%). **D** Fluorescence spectra of H_2O_2/TA system with different FeCo-ONS concentrations (0, 3, 5 μg/mL). Conditions: 0.1 mM TA, 10 mM H_2O_2, λex = 315 nm, and λem = 426 nm

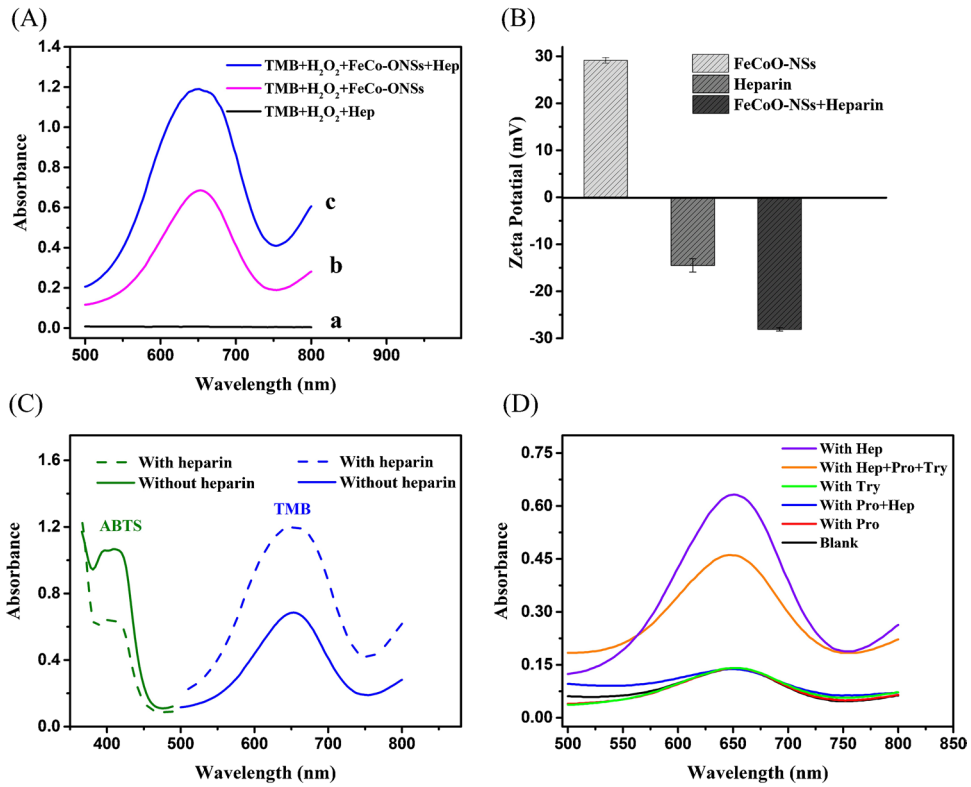

Fig. 3 **A** UV–vis absorption spectra of TMB/H_2O_2 after the addition of (a) heparin, (b) FeCo-ONSs, and (c) heparin and FeCo-ONSs. (**B**) Zeta potential of FeCo-ONSs (25 μg/mL), heparin (10 μg/mL), and FeCo-ONSs (25 μg/mL) + heparin (40 μg/mL). The error bars were obtained from three parallel test results. **C** Effect of heparin on the peroxidase-like activity of FeCo-ONSs toward TMB and ABTS. Conditions: 0.2 mM TMB, 0.2 mM ABTS, 10 mM H_2O_2, 10 μg/mL heparin, 25 μg/mL FeCo-ONSs, and pH 3.5. **D** UV–vis absorption spectra of TMB/H_2O_2/FeCo-ONSs, TMB/H_2O_2/FeCo-ONSs + protamine, TMB/H_2O_2/FeCo-ONSs + protamine + heparin, TMB/H_2O_2/FeCo-ONSs + trypsin, TMB/H_2O_2/FeCo-ONSs + protamine + heparin + trypsin, and TMB/H_2O_2/FeCo-ONSs + heparin

c). The control experiment demonstrates that heparin itself could not catalyze the oxidation of TMB (curve a). The affinity of catalyst toward substrates directly affects the efficiency of catalytic reaction. Heparin, a sulfated polysaccharide, has been widely used as an essential clinical anticoagulant for many years [46]. Negatively charged heparin could be

adsorbed to the surface of FeCo-ONSs by electrostatic interaction between the FeCo-ONSs and heparin. The addition of heparin made the surface charge of FeCo-ONSs highly negative, thus the FeCo-ONSs would have increased affinity towards TMB containing two amine groups by electrostatic attraction. For deeply understanding the mechanism of this heparin-induced catalysis enhancement, a series of experiments were carried out. First of all, the zeta potentials of FeCo-ONSs with and without heparin were performed. As illustrated in Fig. 3(B), the zeta potential of heparin was − 14.5 mV, confirming the negatively charged feature of heparin. The zeta potential of FeCo-ONSs varied from 29.1 mV to − 28.1 mV after adding heparin. This considerable transformation of surface charge property proved that the negatively charged heparin was adsorbed onto the positively charged FeCo-ONSs and the surface of FeCo-ONSs became negative. Contrary to TMB, another typical substrate ABTS with two sulfonic acid groups is negatively charged [23, 47]. Figure 3(C) shows that the peroxidase-like activity of FeCo-ONSs toward ABTS was weakened after adding heparin. The results of above comparative experiments indicated that the electrostatic interaction between FeCo-ONSs and substrates played a significant part in adjusting catalytic activity.

Furthermore, the steady-state kinetics of FeCo-ONSs with heparin was also studied to explore this peroxidase-like activity enhancement. The Michaelise-Menten curves and Lineweaver–Burk plots with and without heparin are shown in Fig. S2, and the comparison of kinetic parameters of FeCo-ONSs in the absence and presence of heparin are given in Table S1. As listed in Table S1, the K_m value of FeCo-ONSs with TMB as substrate in the presence of heparin was lower than that without heparin, verifying the FeCo-ONSs-heparin had a stronger affinity toward TMB. According to the above results, the mechanism of this heparin-induced catalysis enhancement can be explained as follows: the adsorbed heparin modulated the surface charge of FeCo-ONSs and further improved the affinity toward TMB, resulting in the increment of catalytic ability of the FeCo-ONSs.

Protamine sulfate is known as a clinical antagonist to heparin and is used routinely after cardiac and vascular surgery to reverse the anticoagulant function of heparin [48]. It has been reported that the polycationic protamine could bind polyanionic heparin via an electrostatic interaction to form a stable complex [49]. Hence, the heparin would preferentially combine protamine and desorb from the surface of the FeCo-ONSs in the presence of protamine, leading to a decrease in catalysis activity of FeCo-ONSs. However, protamine rich in basic arginine residues could be hydrolyzed into small fragments by trypsin. As a result, the heparin failed to combine with protamine and the enhancement of POD-like activity of FeCo-ONSs was recovered accompanied by the increase of absorbance of oxTMB. Consequently, the trypsin concentration could be quantified according to the absorbance value at 652 nm.

To assess the feasibility of this developed sensing platform for trypsin determination, the effect of various substances contained in system on the detection was investigated. It can be seen in Fig. 3(D) that the absorbance of the FeCo-ONSs/TMB/H_2O_2 system had no obvious change in the presence of individual protamine or trypsin, which suggested that protamine or trypsin had no effect on the peroxidase-like activity of FeCo-ONSs. The absorbance of oxTMB was decreased when protamine was added in the FeCo-ONSs/heparin/TMB/H_2O_2 system. After the trypsin was incubated with protamine and added into TMB/H_2O_2/FeCo-ONSs/heparin system, the absorption peak of oxTMB restored. The above results revealed that our method was feasible for the determination of trypsin.

Detection of trypsin and selectivity

To obtain the sensitive detection performance, some vital factors were optimized systematically. Full details were given in supporting information. Under the optimal conditions, a colorimetric detection was implemented by recording the absorbance at 652 nm of designed sensing system. As shown in Fig. 4(A), the absorbance intensity at 652 nm of the designed colorimetric system increased with the increasing of trypsin concentration. A superior linear relationship between the absorbance and trypsin concentration in the range of 5–500 ng/mL was exhibited in the inset of Fig. 4(B), followed the regression equation of $A = 3.181 \times 10^{-4}[\text{Trypsin}] + 0.104$ ($R^2 = 0.997$) and a limit of detection (LOD) of 2.8 ng/mL (LOD = 3σ/k, where σ is the standard deviation for the blank solution, and k is the slope of the absorbance intensity versus the logarithm of trypsin concentration). Moreover, Table S2 summarizes some comparisons for the determination of trypsin based on different technologies and materials. Satisfactorily, our colorimetric method has the lower detection limit as well as a wide linear range.

Besides sensitivity, selectivity and anti-interference are two other critical parameters to evaluate the practicability of our assay method in a relatively complex biological environment. Some common ions (Na^+, K^+, Mg^{2+}, Ca^{2+}, Cl^-, SO_4^{2-}), amino acids (tryptophan, threonine, phenylalanine), biomolecules (glucose, urea), and bio-enzymes (pepsin, papain, glucose oxidase, urease) were chosen to assess the selectivity and anti-interference of this sensing platform. Figure 5(A) illustrates that the absorbance value only exhibited a remarkable increase when trypsin (500 ng/mL) was present; even the concentrations of other substances were ten times of that of trypsin, indicating a good selectivity of this colorimetric sensing strategy for the determination of trypsin. Figure 5(B) displays that the absorbance intensity kept basically unchanged after introducing the interfering

substances in the presence of trypsin, which illustrated good anti-interference performance of this method.

Trypsin analysis in real samples

For further investigating the applicability of our colorimetric method for trypsin determination in real sample, standard addition method was performed to detect trypsin in healthy human urine samples and multienzyme tablets samples. According to the previous reports [50], there is almost no trypsin in urine of healthy people. As shown in Table 1, no trypsin was found in the healthy urine samples. The average recoveries of trypsin in the human urine samples were ranging from 95.0 to 104.8%, and the relative standard deviation (RSD) was no more than 3.4%, suggesting this method is feasible and reliable for measuring trypsin activity in urine samples.

Multienzyme tablet containing trypsin and some other digestive enzymes is used to help treat indigestion. The national drug standards stipulate that trypsin activity should not be less than 160 U per tablet. Considering this high trypsin level and the linear range of our method,

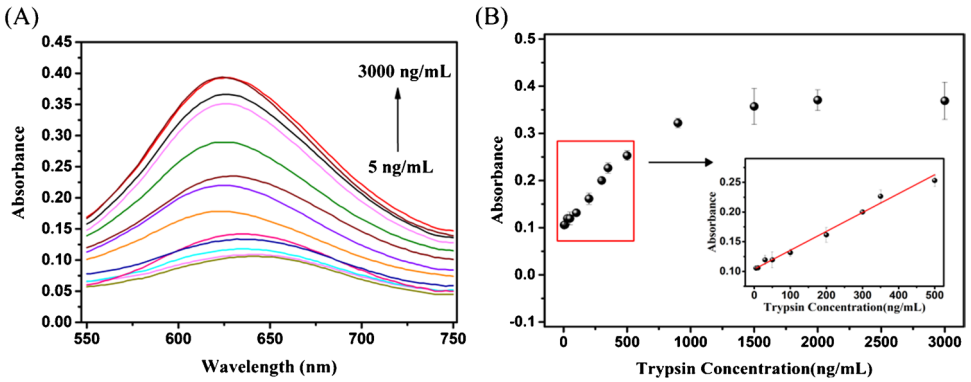

Fig. 4 **A** UV–vis absorption spectra of FeCo-ONSs/heparin/protamine/H_2O_2/TMB sensing system with different trypsin concentrations (5, 10, 50, 100, 200, 300, 350, 500, 900, 1500, 2000, 3000 ng/mL). **B** Relationship between the absorbance at 652 nm and trypsin concentration (5–3000 ng/mL). Inset: the linear range of calibration curve of the absorbance at 652 nm versus trypsin concentration (5–500 ng/mL). The error bars were obtained from three parallel test results

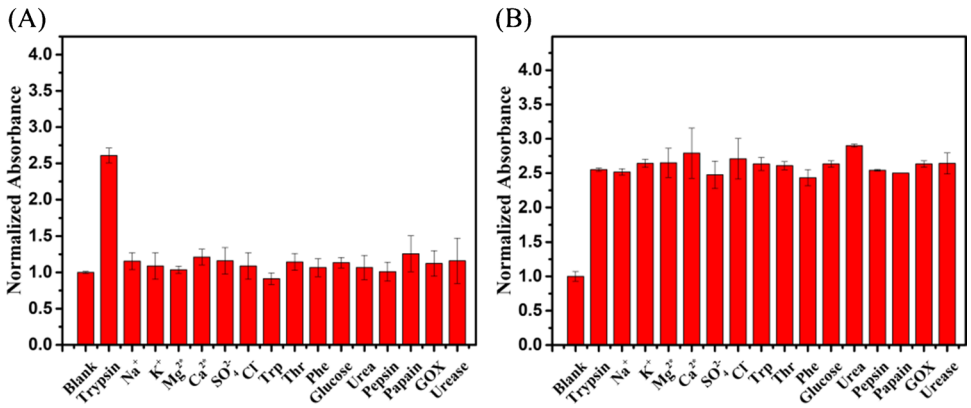

Fig. 5 The selectivity (**A**) and interference (**B**) analysis of the FeCo-ONSs/H_2O_2/TMB/heparin/protamine system for detection of trypsin over potential interfering substances (the concentrations of other substances were ten times of that of trypsin)

Table 1 Determination of trypsin in real samples

Samples	Human urine samples				Multienzyme tablet samples			
	Added (ng/mL)	Found (ng/mL)	Recovery (%)	RSD (%, $n=3$)	Added (ng/mL)	Found (ng/mL)	Recovery (%)	RSD (%, $n=3$)
1	0	-	-	-	0	230.5	-	3.2
2	50.0	52.4	104.8	3.4	50.0	276.6	98.6	2.3
3	100.0	104.8	104.8	3.4	100.0	332.2	100.5	1.4
4	150.0	142.5	95.0	2.5	150.0	368.9	97.0	3.4

multienzyme tablet samples with three trypsin-spiked concentrations (200, 400, 600 μg/mL) were diluted 4000 times for further detection. As shown in Table 1, 230.5 ng/mL of trypsin was found in diluted multienzyme tablet samples. After calculation, the trypsin content of a multienzyme tablet was 0.9 mg (230 U) which conformed to the related stipulation. The average recoveries of trypsin in multienzyme tablet samples were ranging from 97.0 to 100.5%, and the RSD was no more than 3.4%. The above results illustrated our method had good practicability for trypsin determination in real samples. However, our method has some limitations such as the low solubility of FeCo-ONSs and possible electrostatic interference in more complex clinical samples. Hence, further research is still required to improve the solubility of nanozymes and the specificity of the assay.

Conclusion

In this work, the 2D FeCo-ONSs with peroxidase mimetic activity were synthesized by using a solution reduction method. The heparin-adsorbed FeCo-ONSs showed higher peroxidase-like activity due to stronger affinity toward substrate caused by electrostatic interaction. Moreover, a novel and sensitive colorimetric assay for trypsin was established based on the peroxidase-like activity enhancement of FeCo-ONSs, which provided a wider linear in the range of 5–500 ng/mL and a lower detection limit of 2.8 ng/mL. The proposed method was applied for determination of trypsin in human urine and drug samples, which exposed the tremendous feasibility for offering a potential method for trypsin detection in complex real samples. In addition, this finding brings valuable insights into regulating nanozyme activities through controlling the surface charge of the nanozymes, and might be extended to increase the activity of other 2D nanozymes.

Supplementary Information The online version contains supplementary material available at https://doi.org/10.1007/s00604-022-05227-3.

Acknowledgements This work is supported by the National Natural Science Foundation of China (No. 21775052 and No. 21575048) and the Science and Technology Development project of Jilin province, China (No. 20180414013GH).

Declarations

Ethics approval and consent to participate All experiments were performed in compliance with the relevant laws and institutional guidelines, and the writing of informed consent for all samples was obtained from human subjects.

Conflict of interest The authors declare no competing interests.

References

1. Ou L-J, Li X-Y, Li L-J, Liu H-W, Sun A-M, Liu K-J (2015) A sensitive assay for trypsin using poly(thymine)-templated copper nanoparticles as fluorescent probes. Analyst 140:1871–1875. https://doi.org/10.1039/c4an01994f
2. Kim KK, Turner R, Khazan N, Kodza A, Jones A, Singh RK, Moore RG (2020) Role of trypsin and protease-activated receptor-2 in ovarian cancer. PLoS ONE 15:e0232253. https://doi.org/10.1371/journal.pone.0232253
3. Yan J, Xie C, Zhu J, Song Z, Wang Z, Li L (2021) Effect of trypsin concentration on living SMCC-7721 cells studied by atomic force microscopy. J Microsc. https://doi.org/10.1111/jmi.13053
4. Shi Y, Jiang Y, Sui D, Li Y, Chen T, Ma L, Ding Z (1996) Affinity chromatography of trypsin using chitosan as ligand support. J Chromatogr A 742:107–112
5. Braatz JA, Elias C, Finny JG, Tran H, McCaman M (2015) Quantitation of residual trypsin in cell-based therapeutics using immobilized α-1-antitrypsin or SBTI in an ELISA format. J Immunol Methods 417:131–133. https://doi.org/10.1016/j.jim.2014.12.009
6. Zhou Z, Liu W, Wang Y, Ding F, Liu X, Zhao Q, Zou P, Wang X, Rao H (2019) A fluorometric and colorimetric method for determination of trypsin by exploiting the gold nanocluster-induced aggregation of hemoglobin-coated gold nanoparticles. Mikrochim Acta 186:272. https://doi.org/10.1007/s00604-019-3380-2
7. Poon C-Y, Li Q, Zhang J, Li Z, Dong C, Lee AW-M, Chan W-H, Li H-W (2016) FRET-based modified graphene quantum dots for direct trypsin quantification in urine. Anal Chim Acta 917(64–70):10
8. Liu H, Yin H, Dong Y, Ding H, Chu X (2020) Electrochemiluminescence resonance energy transfer between luminol and black phosphorus nanosheets for the detection of trypsin via the "off-on-off" switch mode. Analyst 145:2204–2211. https://doi.org/10.1039/d0an00156b1016/j.aca.2016.02.032
9. Zhang H, Yu D, Zhao Y, Fan A (2014) Turn-on chemiluminescent sensing platform for label-free protease detection using streptavidin-modified magnetic beads. Biosens Bioelectron 61:45–50. https://doi.org/10.1016/j.bios.2014.04.050
10. Zhang H, Yao L, Yu X, Zhao Y, Fan A (2015) Graphene oxide-based chemiluminescent sensing platform for label-free detection of trypsin and its inhibitors. Anal Methods 7:9949–9956. https://doi.org/10.1039/C5AY02038G
11. Chen L, Fu X, Li J (2013) Ultrasensitive surface-enhanced Raman scattering detection of trypsin based on anti-aggregation of 4-mercaptopyridine-functionalized silver nanoparticles: an optical sensing platform toward proteases. Nanoscale 5:5905–5911. https://doi.org/10.1039/c3nr00637a
12. He Y, Li N, Liu X, Chen W, Zhu X, Liu Q (2021) 5,10,15,20-tetrakis (4-carboxyl phenyl) porphyrin-functionalized urchin-like CuCo2O4 as an excellent artificial nanozyme for determination of dopamine. Mikrochim Acta 188:171. https://doi.org/10.1007/s00604-021-04819-9
13. Wang X, Shi Q, Zha Z, Zhu D, Zheng L, Shi L, Wei X, Lian L, Wu K, Cheng L (2021) Copper single-atom catalysts with photothermal performance and enhanced nanozyme activity for bacteria-infected wound therapy. Bioactive materials 6:4389–4401. https://doi.org/10.1016/j.bioactmat.2021.04.024
14. Wu C-Y, Hsu Y-H, Chen Y, Yang L-C, Tseng S-C, Chen W-R, Huang C-C, Wan D (2021) Robust O2 supplementation from a trimetallic nanozyme-based self-sufficient complementary system synergistically enhances the starvation/photothermal therapy against hypoxic tumors. ACS Appl Mater Interfaces 13:38090–38104. https://doi.org/10.1021/acsami.1c10656
15. Koyappayil A, Kim HT, Lee M-H (2021) 'Laccase-like' properties of coral-like silver citrate micro-structures for the degradation

and determination of phenolic pollutants and adrenaline. J Hazard Mater 412:125211. https://doi.org/10.1016/j.jhazmat.2021.125211
16. Huang H, Li M, Hao M, Yu LL, Li Y (2021) A novel selective detection method for sulfide in food systems based on the GMP-Cu nanozyme with laccase activity. Talanta 235:122775. https://doi.org/10.1016/j.talanta.2021.122775
17. Gao L, Zhuang J, Nie L, Zhang J, Zhang Y, Gu N, Wang T, Feng J, Yang D, Perrett S, Yan X (2007) Intrinsic peroxidase-like activity of ferromagnetic nanoparticles. Nat Nanotechnol 2:577–583
18. Li P, Wu C, Xu Y, Cheng D, Lu Q, Gao J, Yang W, Zhu X, Liu M, Li H, Yin P, Zhang Y (2020) Group IV nanodots: newly emerging properties and application in biomarkers sensing. TrAC, Trends Anal Chem 131:116007. https://doi.org/10.1016/j.trac.2020.116007
19. Shi W, Wang Q, Long Y, Cheng Z, Chen S, Zheng H, Huang Y (2011) Carbon nanodots as peroxidase mimetics and their applications to glucose detection. Chem Commun 47:6695–6697. https://doi.org/10.1039/c1cc11943e
20. Guo J, Wu S, Wang Y, Zhao M (2020) A label-free fluorescence biosensor based on a bifunctional MIL-101(Fe) nanozyme for sensitive detection of choline and acetylcholine at nanomolar level. Sens Actuat B Chem 312:128021. https://doi.org/10.1016/j.snb.2020.128021
21. Xie J, Cheng D, Li P, Xu Z, Zhu X, Zhang Y, Li H, Liu X, Liu M, Yao S (2021) Au/metal–organic framework nanocapsules for electrochemical determination of glutathione. ACS Appl Nano Mater 4:4853–4862. https://doi.org/10.1021/acsanm.1c00394
22. Yang L, Liu X, Lu Q, Huang N, Liu M, Zhang Y, Yao S (2016) Catalytic and peroxidase-like activity of carbon based-AuPd bimetallic nanocomposite produced using carbon dots as the reductant. Anal Chim Acta 930:23–30. https://doi.org/10.1016/j.aca.2016.04.041
23. Chen C, Zhao D, Jiang Y, Ni P, Zhang C, Wang B, Yang F, Lu Y, Sun J (2019) Logically regulating peroxidase-like activity of gold nanoclusters for sensing phosphate-containing metabolites and alkaline phosphatase activity. Anal Chem 91(23):15017–15024. https://doi.org/10.1021/acs.analchem.9b03629
24. Du Z, Wei C (2020) Using G-Rich sequence to enhance the peroxidase-mimicking activity of DNA-Cu/Ag nanoclusters for rapid colorimetric detection of hydrogen peroxide and glucose. Chem Select 5(17):5166–5171. https://doi.org/10.1002/slct.202000956
25. Liang X, Han L (2020) White peroxidase-mimicking nanozymes: colorimetric pesticide assay without interferences of O_2 and color. Adv Funct Mater 30(28):2001933. https://doi.org/10.1002/adfm.202001933
26. Zhu Y, Zhang Z, Song X, Bu Y (2021) A facile strategy for synthesis of porous Cu_2O nanospheres and application as nanozymes in colorimetric biosensing. J Mater Chem B 9(16):3533–3543. https://doi.org/10.1039/d0tb03005h
27. Xu Y, Li P, Hu X, Chen H, Tang Y, Zhu Y, Zhu X, Zhang Y, Liu M, Yao S (2021) Polyoxometalate nanostructures decorated with CuO nanoparticles for sensing ascorbic acid and Fe 2+ ions. ACS Appl Nano Mater 4:8302–8313. https://doi.org/10.1021/acsanm.1c01495
28. Swaidan A, Borthakur P, Boruah PK, Das MR, Barras A, Hamieh S, Toufaily J, Hamieh T, Szunerits S, Boukherroub R (2019) A facile preparation of CuS-BSA nanocomposite as enzyme mimics: application for selective and sensitive sensing of Cr(VI) ions. Sens Actuat B Chem 294:253–262. https://doi.org/10.1016/j.snb.2019.05.052
29. Song Y, Qu K, Zhao C, Ren J, Qu X (2010) Graphene oxide: intrinsic peroxidase catalytic activity and its application to glucose detection. Adv Mater 22(19):2206–2210. https://doi.org/10.1002/adma.200903783
30. Wang T, Bai Q, Zhu Z, Xiao H, Jiang F, Du F, Yu WW, Liu M, Sui N (2021) Graphdiyne-supported palladium-iron nanosheets: a dual-functional peroxidase mimetic nanozyme for glutathione detection and antibacterial application. Chem Eng J 413:127537. https://doi.org/10.1016/j.cej.2020.127537
31. Wu J, Yang Q, Li Q, Li H, Li F (2021) Two-dimensional MnO2 nanozyme-mediated homogeneous electrochemical detection of organophosphate pesticides without the interference of H_2O_2 and color. Anal Chem 93(8):4084–4091. https://doi.org/10.1021/acs.analchem.0c05257
32. Wei X, Chen J, Ali MC, Munyemana JC, Qiu H (2020) Cadmium cobaltite nanosheets synthesized in basic deep eutectic solvents with oxidase-like, peroxidase-like, and catalase-like activities and application in the colorimetric assay of glucose. Mikrochim Acta 187(6):314. https://doi.org/10.1007/s00604-020-04298-4
33. Zhao Q, Shen T, Liu Y, Hu X, Zhao W, Ma Z, Li P, Zhu X, Zhang Y, Liu M, Yao S (2021) Universal nanoplatform for formaldehyde detection based on the oxidase-mimicking activity of MnO2 nanosheets and the in situ catalysis-produced fluorescence species. J Agric Food Chem 69:7303–7312. https://doi.org/10.1021/acs.jafc.1c01174
34. Hong C, Chen L, Wu C, Yang D, Dai J-Y, Huang Z, Cai R, Tan W (2022) Green synthesis of Au@WSe2 hybrid nanostructures with the enhanced peroxidase-like activity for sensitive colorimetric detection of glucose. Nano Res 15:1587–1592. https://doi.org/10.1007/s12274-021-3706-3
35. Ma D, Yu J, Yin W, Zhang X, Mei L, Zu Y, An L, Gu Z (2018) Synthesis of surface-modification-oriented nanosized molybdenum disulfide with high peroxidase-like catalytic activity for H2O2 and cholesterol detection. Chem-Eur J 24(59):15868–15878
36. Zhuang L, Ge L, Yang Y, Li M, Jia Y, Yao X, Zhu Z (2017) Ultrathin iron-cobalt oxide nanosheets with abundant oxygen vacancies for the oxygen evolution reaction. Adv Mater 29(17):1606793. https://doi.org/10.1002/adma.201606793
37. Wu X, Wang W, Li F, Khaimanov S, Tsidaeva N, Lahoubi M (2016) PEG-assisted hydrothermal synthesis of CoFe2O4 nanoparticles with enhanced selective adsorption properties for different dyes. Appl Surf Sci 389:1003–1011. https://doi.org/10.1016/j.apsusc.2016.08.053
38. Nie M, Li Y, Li L, He J, Hong P, Zhang K, Cai X, Kong L, Liu J (2021) Ultrathin iron-cobalt oxide nanosheets with enhanced H_2O_2 activation performance for efficient degradation of tetracycline. Appl Surf Sci 535:147655. https://doi.org/10.1016/j.apsusc.2020.147655
39. Li X-H, Xu C-L, Han X-H, Qiao L, Wang T, Li F-S (2010) Synthesis and magnetic properties of nearly monodisperse CoFe2O4 nanoparticles through a simple hydrothermal condition. Nanoscale Res Lett 5(6):1039–1044. https://doi.org/10.1007/s11671-010-9599-9
40. Wang M, Zhou X, Wang S, Xie X, Wang Y, Su X (2021) Fabrication of bioresource-derived porous carbon-supported iron as an efficient oxidase mimic for dual-channel biosensing. Anal Chem 93(6):3130–3137. https://doi.org/10.1021/acs.analchem.0c04386
41. Liu Y, Zhou M, Cao W, Wang X, Wang Q, Li S, Wei H (2019) Light-responsive metal-organic framework as an oxidase mimic for cellular glutathione detection. Anal Chem 91(13):8170–8175
42. Liu C, Cai Y, Wang J, Liu X, Ren H, Yan L, Zhang Y, Yang S, Guo J, Liu A (2020) Facile preparation of homogeneous copper nanoclusters exhibiting excellent tetraenzyme mimetic activities for colorimetric glutathione sensing and fluorimetric ascorbic acid sensing. ACS Appl Mater Interfaces 12(38):42521–42530. https://doi.org/10.1021/acsami.0c11983
43. Li H, Li J, Ai Z, Jia F, Zhang L (2018) Oxygen vacancy-mediated photocatalysis of BiOCl: reactivity, selectivity, and perspectives. Angew Chem 57(1):122–138. https://doi.org/10.1002/anie.201705628
44. Huang L, Niu Y, Li R, Liu H, Wang Y, Xu G, Li Y, Xu Y (2019) VO x quantum dots with multienzyme-mimic activities and the

application in constructing a three-dimensional (3D) coordinate system for accurate discrimination of the hydrogen peroxide over a broad concentration range. Anal Chem 91(9):5753–5761. https://doi.org/10.1021/acs.analchem.8b05923
45. Gong F, Yang N, Wang Y, Zhuo M, Zhao Q, Wang S, Li Y, Liu Z, Chen Q, Cheng L (2020) Oxygen-deficient bimetallic oxide FeWOX nanosheets as peroxidase-like nanozyme for sensing cancer via photoacoustic imaging. Small 16(46):e2003496. https://doi.org/10.1002/smll.202003496
46. He S-B, Zhuang Q-Q, Yang L, Lin M-Y, Kuang Y, Peng H-P, Deng H-H, Xia X-H, Chen W (2020) A heparinase sensor based on a ternary system of Hg^{2+}-heparin-osmium nanoparticles. Anal Chem 92(1):1635–1642. https://doi.org/10.1021/acs.analchem.9b05222
47. Liu Y, Ding D, Zhen Y, Guo R (2017) Amino acid-mediated 'turn-off/turn-on' nanozyme activity of gold nanoclusters for sensitive and selective detection of copper ions and histidine. Biosens Bioelectron 92:140–146. https://doi.org/10.1016/j.bios.2017.01.036
48. Amro M, Mansoor K, Amro A, Okoro K, Okhumale PI (2020) Kounis syndrome induced by protamine sulfate. Cureus 12(2):e6972
49. Carr JA, Silverman N (1999) The heparin-protamine interaction-a review. J Cardiovasc Surg 40(5):659–666
50. See WA, Smith JL (1991) Urinary levels of activated trypsin in whole-organ pancreas transplant patients with duodenocystostomies. Transplantation 52:630–633